*Article*

# Spatio-Temporal Patterns of Land-Use Changes and Conflicts between Cropland and Forest in the Mekong River Basin during 1990–2020

**Jiahao Zhai [1], Chiwei Xiao [2,3,*], Zhiming Feng [2,3,4] and Ying Liu [1]**

[1] School of Geography and Environment, Jiangxi Normal University, Nanchang 330022, China; zhaijh@jxnu.edu.cn (J.Z.); liuy64@jxnu.edu.cn (Y.L.)
[2] Institute of Geographic Sciences and Natural Resources Research, Chinese Academy of Sciences, Beijing 100101, China; fengzm@igsnrr.ac.cn
[3] College of Resources and Environment, University of Chinese Academy of Sciences, Beijing 100049, China
[4] Key Laboratory of Carrying Capacity Assessment for Resource and Environment, Ministry of Natural Resources, Beijing 101149, China
[*] Correspondence: xiaocw@igsnrr.ac.cn

**Abstract:** The Mekong River Basin (MRB) has experienced drastic and extensive land-use and land-cover changes (LULCCs) since the 1990s, including the conflicts between cropland and forest, yet remain quantitatively uninvestigated. With three decades (1990–2020) of land-use products, here we reveal the characteristics of LULCCs and the conflicts between cropland and forest in the MRB and its three sub-basins, i.e., upstream area (UA), midstream area (MA), and downstream area (DA). The four main results are as follows: (1) Since 1990, the dominated features are forest loss and cropland expansion in the MRB and show obvious sub-basin differences. (2) The LULCC was most active before 2000, with a comprehensive dynamic degree of almost 2%. Among them, construction land has the highest single dynamic degree (5%), especially in the DA, reaching 12%. (3) The key features of land-use transfer are the interconversions of forest and cropland, as well as cropland converted into construction land. About 18% (63,940 km$^2$) of forest was reclaimed as cropland, and 17% (45,967 km$^2$) of cropland was returned to forest in the past 31 years. (4) The conflict between cropland and forest was the most dominant LULCC, accounting for 86% of the MRB area. Overall, cropland expansion and forest loss (CEFL) were more dominant in the DA, while cropland fallow and forest restoration (CFFR) had an advantage in the MA. Indeed, CEFL was mainly seen in the plains below a 200 m elevation level, while CFFR tended to occur in the highlands. Our basin-scale study can enrich the existing pan-regional results of LULCCs, and facilitates the understanding of the dynamics and related mechanisms of CFER and CFFR in the tropics.

**Keywords:** land-use and land-cover changes (LULCCs); cropland expansion; forest loss; spatio-temporal characteristics; the Mekong river basin (MRB)

## 1. Introduction

Land-use and land-cover changes (LULCCs) are among the most prominent landscape effects on Earth, and they are also an important cause and critical consequence of global climate change [1]. LULCCs, particularly deforestation and/or forest transformation, often cause a series of adverse effects, such as land degradation, biodiversity loss, reduction in clean water resources, increased carbon emissions, and air pollution [2–8], and they may reduce the value of ecosystem services and enhance ecological risks [9,10]. To prevent and reverse unreasonable land use, some ongoing global initiatives, such as Sustainable Development Goals (SDGs) [11] and Reducing Emissions from Deforestation and Forest Degradation projects (REDD+) [12], are committed to protecting and restoring sustainable terrestrial ecosystems. Therefore, mastering the process and characteristics of LULCCs,

especially forest degradation or transformation due to agricultural expansion and intensification, has a positive effect on the reasonable policy formulation of land use on global and regional scales.

To date, numerous scholars, governments, and international social groups have paid attention to LULCCs [13–15]. LULCCs are widely involved in a series of major issues, including the effective development and reasonable use of resources, ecological and environmental protection and governance, food production and security, and sustainable development of the social economy [16]. The present research on LULCCs mainly includes dynamic monitoring, spatio-temporal processes, driving factors, and environmental impacts [17,18]. Regarding the processes of LULCCs, they have witnessed the quantity and degree of changes, the direction of transfer, and the spatial patterns [19]. Because LULCCs in different regions have different contributions and responses to global changes, regional-scale LULCC studies tend to focus on key regions and hot spots, such as megacities and watersheds [20–22]. As a complete natural geographical unit, a river basin is crucial to human survival and sustainable social and economic development. Generally, LULCCs in river basins are more dramatic than those in other regions [23–25]. The driving forces that trigger LULCCs in river basins are complicated, among which economic development, human activities, and population growth are the most important [26,27].

The Mekong River is the mother river of Mainland Southeast Asia (MSEA); its basin area covers most of Laos and Cambodia and parts of Myanmar, Thailand, and Vietnam, accounting for approximately one-third of the total area of MSEA. The Asian Development Bank launched the Greater Mekong Subregional Cooperation initiative in 1992, with participants including China and MSEA's five countries. The aim was to strengthen economic ties among its members and to promote peace and prosperity in the subregion [28]. Since the 1990s, the Mekong River Basin (MRB) has experienced rapid economic growth and, as population growth has put pressure on natural resources, this growth has significantly contributed to the rate of LULCCs, including forest loss and agricultural expansion [29,30]. Additionally, earlier studies have shown that urban expansion, road construction, rubber plantations boom, and illegal logging have led to forest loss and regrowth or degradation in the MRB [31–34]. These changes have resulted in a decline in water quality, with severe hydrological consequences, and significant impacts on the largest lake (i.e., Tonle Sap Lake) in the watersheds [35–37]. In addition, LULCCs are the main drivers of basin runoff changes and can also alter soil properties [38–40]. Although previous studies have considerably enriched our understanding of LULCCs, the magnitudes, processes, and characteristics of LULCCs at the basin scale (e.g., the MRB) are still understudied, especially in the quantitative analysis of the conflicts between cropland and forest.

Based on 30 m land-use and digital elevation model (DEM) data products, here, we use the dynamic degree and transfer matrix method to delineate LULCCs in the MRB during 1990–2020. The objective of this study is two-fold: (1) to reveal the dynamic processes and spatial patterns of LULCCs in the MRB over the past 31 years; and (2) to analyze the characteristics of conflicts between cropland and forest, including elevation trends. Understanding the process of LULCCs and cropland expansion or fallow and forest loss or restoration in the MRB since 1990 can provide support and practice for future regional land-use management and structure optimization, and will facilitate the understanding of the dynamics and related mechanisms of LUCCs in the tropics.

## 2. Materials and Methods

### 2.1. Study Area

The Mekong River, or Chinese Lancang River, originates from the northeast slope of the Tanggula Mountains on the Tibetan Plateau. The Mekong River is the most important transnational river system in Asia and the longest river in MSEA, flowing through Laos, Myanmar, Thailand, Cambodia, and Vietnam, with a total length of 2668 km. The Mekong River Basin (MRB) is located 99° E–108° E and 8° N–22° N, with a total area of 655,281 km$^2$. The MRB has a typical tropical monsoon climate, with both dry and rainy seasons in the year.

The rainy season is from June to October and the dry season is from November to May of the following year. The topography of the MRB is high in the north and low in the middle and south (Figure 1a). According to previous studies [41,42], we divided the MRB into three sub-basins, namely, the upstream area (UA), midstream area (MA), and downstream area (DA) (Figure 1b). The overall population distribution of the MRB is sparse in the north and dense in the south, especially in the DA delta with the highest density.
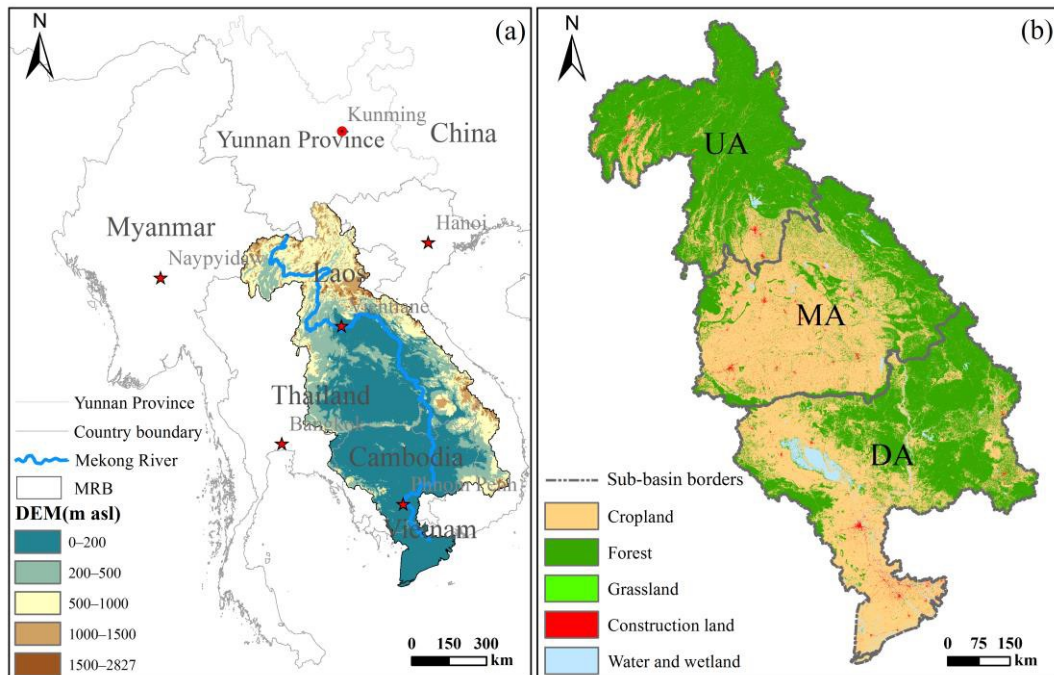


**Figure 1.** The maps of (**a**) the Mekong River Basin (MRB) and its topography (Advanced Spaceborne Thermal Emission and Reflection Radiometer Global Digital Elevation Model Version 3; ASTER GDEM V3) showing the (**b**) land use in 2020; UA, MA, and DA represent the upstream, midstream, and downstream areas of the MRB, respectively.

Cropland and forest are the main types of land use and land cover in the MRB (Figure 1b). Based on land-use data for 2020, the area of cropland and forest in the MRB is nearly 629,076 km$^2$, accounting for more than 96% of the total basin. More specially, croplands are mainly distributed in the MA (46%) and DA (44%), and forests are mainly distributed in the UA (41%) and DA (36%). The area of construction land is about 9396 km$^2$, accounting for merely 1% of the MRB's totality. The area of grassland is nearly 250 km$^2$, which is mainly distributed in the UA (56%) and MA (41%). Due to the Tonle Sap Lake, more than 70% of the water and wetlands of the MRB are located in the DA.

### 2.2. Data Sources

#### 2.2.1. Land-Use Data Products

The land-use data were obtained from the Big Earth Data Science Engineering Program of the Chinese Academy of Sciences Strategic Priority Research Program (https://data.casearth.cn, latest access: 10 September 2021). These data were based on Landsat satellite data (Landsat TM, ETM+, and OLI) from 1984 to 2020. For more information about land-use data products, one can refer to the study conducted by Zhang and colleagues [43]. The land-use types of the original data were classified into 9 level-0 land-cover categories (i.e., cropland, forest, shrubland, grassland, wetlands, impervious surfaces, bare areas, water body, permanent ice and snow) and 16 level-1 categories. The accuracy of the 30 m resolution level-0-type dataset was greater than 82.5% [43], which can meet the data requirements of this study. To better illustrate the spatio-temporal characteristics of LULCCs and conflicts between cropland and forest, we re-classified land-cover types into

five classes (i.e., cropland, forest, grassland, construction land, and water and wetland). In other words, the forest and shrubland land covers reclassified as forest, water body, and wetlands were merged into water and wetland, construction land referred to impervious surfaces, and cropland and grassland remained unchanged. It should be pointed out that bare areas and permanent ice and snow were nearly non-existent in the MRB and therefore not included in this study.

### 2.2.2. ASTER GDEM V3 Data Products

The Advanced Spaceborne Thermal Emission and Reflection Radiometer Global Digital Elevation Model Version 3 (ASTER GDEM V3) was obtained from the Earth Data open access website (https://earthdata.nasa.gov, latest access: 13 March 2022). ASTER GDEM was developed by the U.S. National Aeronautics and Space Administration (NASA) and the Japanese Ministry of Economy, Trade and Industry (METI). On 5 August 2019, NASA and METI jointly released ASTER GDEM V3, which added 360,000 optical stereo pairs to V2 to reduce elevation blank areas and water-area numerical anomalies. ASTER GDEM V3 is a 30 m high-definition DEM that covers almost all of Earth's land. It takes 97 tiles to cover the MRB, and then mosaicked in ArcGIS 10.x to extract the MRB topographical (or elevation) information. Here, GDEM V3 was used to generate the elevational trends of conversion or conflict between cropland and forest in the MRB. According to the standard division of landform units [44,45], and combined with the change characteristics of cropland and forest in the MRB, the elevation was divided into below 200 m (plain), 200–500 m (hill), 500–1000 m (low mountain), and above 1000 m (middle mountain).

### 2.3. Analysis Methods

#### 2.3.1. Dynamic Degree

The land-use dynamic degree can reflect the change speed and amplitude of various land-use types in the study area during a period of time, which can be calculated as the single dynamic degree or the comprehensive dynamic degree [46].

The mathematical expression of the land-use single dynamic degree is given by:

$$K = \frac{U_b - U_a}{U_a} \times \frac{1}{T} \times 100\% \tag{1}$$

where $K$ is the dynamic degree of a certain land-use type (e.g., cropland) in the study period; $U_a$ and $U_b$ are the quantities of a certain land-use types at the beginning and end of the study period, respectively. $T$ is the length of the research period. When $T$ is set as a year, the value of $K$ is the annual change rate of a certain land-use type in the research region. Here, we only analyzed the single dynamic degree for cropland and forest, as well as construction land.

The mathematical expression of the comprehensive land-use dynamic degree is given by:

$$LC = \frac{\sum_i \Delta LU_{i-j}}{\sum_i LU_i} \times \frac{1}{T} \times 100\% \tag{2}$$

where $LU_i$ is the area of the $i$-th land-use type (e.g., cropland) at the beginning of the research period, $\Delta LU_{i-j}$ represents the area in which the $i$-th land-use type is converted into the $j$-th land-use type during the research period, and $T$ is the length of the monitoring period. When the time period of $T$ is set as a year, the value of $LC$ is the annual change rate of land use in the research region.

#### 2.3.2. Transfer Matrix

The land-use transfer matrix [47] can be obtained as a two-dimensional matrix, according to the change relationships of land-cover status in the same region at different phases.

Through the analysis of the transfer matrix, the conversions of different land types in two phases can be obtained. The mathematical expression of the land-use transfer matrix is:

$$S_{ij} = \begin{bmatrix} S_{11} & S_{12} & \cdots & S_{1n} \\ S_{21} & S_{22} & \cdots & S_{2n} \\ \cdots & \cdots & \cdots & \cdots \\ S_{n1} & S_{n2} & \cdots & S_{nn} \end{bmatrix} \tag{3}$$

where $S$ represents the area (km$^2$); $n$ represents the number of land-use types before and after the transfer; $i, j$ ($i, j$ = 1, 2, ... , $n$) represent the land-use types before and after the transfer, respectively; and $S_{ij}$ represents the area (km$^2$) of land type $i$ converted to land type $j$.

## 3. Results

### 3.1. Dynamic Characteristics of LULCCs in the MRB

During 1990–2020, the MRB and its three sub-basins (i.e., UA, MA, and DA) have undergone an obvious large-scale process of LULCCs and were not distributed equally (Tables 1 and A1). Among them, the construction land and cropland areas continued to increase, whereas the forest area decreased. The grassland increased in general and was concentrated mainly in the UA, but the changes were not obvious because of its small size in the whole area over the past 31 years. Additionally, the area of water and wetland increased significantly in the MA.

**Table 1.** Area change (km$^2$) of land use in the Mekong River Basin (MRB) from 1990 to 2020.

| Region | Land-Use and Land-Cover Types | 1990–2020 | 1990–2000 | 2000–2010 | 2010–2020 |
|---|---|---|---|---|---|
| MRB | Cropland | 11,626.3 | 4482.9 | 1288.8 | 5854.6 |
| | Forest | −19,182.2 | −7391.3 | −3802.4 | −7988.5 |
| | Grassland | 136.2 | 213.9 | −44.6 | −33.1 |
| | Construction land | 5438.2 | 1457.0 | 2101.7 | 1879.5 |
| | Water and wetland | 1980.8 | 1237.4 | 456.4 | 287.0 |
| UA | Cropland | 1561.3 | 1121.2 | 722.7 | −282.6 |
| | Forest | −3268.4 | −1917.8 | −1055.5 | −295.0 |
| | Grassland | 100.0 | 182.7 | −45.5 | −37.2 |
| | Construction land | 1011.8 | 204.9 | 359.2 | 447.6 |
| | Water and wetland | 594.8 | 409.0 | 19.1 | 166.7 |
| MA | Cropland | −6481.8 | −6648.1 | −196.9 | 363.2 |
| | Forest | 3454.4 | 5075.9 | −689.9 | −931.6 |
| | Grassland | 29.4 | 26.0 | 0.7 | 2.7 |
| | Construction land | 1936.9 | 647.4 | 738.6 | 550.9 |
| | Water and wetland | 1061.0 | 898.7 | 147.5 | 14.8 |
| DA | Cropland | 16,546.8 | 10,009.8 | 763.0 | 5774.0 |
| | Forest | −19,368.2 | −10,549.3 | −2057.0 | −6761.9 |
| | Grassland | 6.8 | 5.3 | 0.3 | 1.3 |
| | Construction land | 2489.5 | 604.6 | 1003.9 | 881.0 |
| | Water and wetland | 325.0 | −70.4 | 289.9 | 105.5 |

From 1990 to 2020, the construction land increased from 3957.4 km$^2$ to 9395.6 km$^2$, with an annual growth rate of 3.0%. Representing a 2.4-fold increase in the construction land, the area ratio of construction land increased from 0.6% to 1.4%. During 1990–2000 and 2000–2010, construction land expanded relatively fast, with annual growth rates of 3.2% and 3.3%, respectively. The last period of construction land expansion (2010–2020) was the slowest, with an annual growth rate of 2.3%. At the sub-basin scale, the increased area was the largest in the DA, increasing from 688.5 km$^2$ in 1990 to 3178.0 km$^2$ in 2020 and accounting for 45.8% of the total basin growth. The areas of construction land in the

MA and UA increased by 1936.9 km$^2$ and 1011.8 km$^2$, respectively, which correspondingly accounted for 35.6% and 18.6% of the basin growth.

The cropland area increased by 11,626.3 km$^2$ in the past 31 years in the MRB, and the area ratio increased from 42.0% to 43.8%. The fastest period of cropland expansion occurred during 2010–2020, with an increase of 5854.6 km$^2$, followed by 1990–2000 (4482.9 km$^2$) and 2000–2010 (1288.8 km$^2$). Although the overall trend of cropland increased, this was not the case in the different three sub-basins. The cropland area has continued to increase only in the DA, with a total increase of 16,546.6 km$^2$. Specifically, the increase in cropland in the DA was 1.4 times that of the whole basin, indicating that the area of cropland has significantly decreased in the UA and MA. The main reason was that the cropland area in the MA decreased by 6845.0 km$^2$ from 1990 to 2010, though there was a slight increase (363.2 km$^2$) after 2010. Contrary to the MA, the cropland area in the UA showed a trend of first increasing by 1843.9 km$^2$ from 1990 to 2010 and then decreasing by 282.6 km$^2$ since 2010.

From 1990 to 2020, the area of forest loss in the MRB has reached nearly 20,000 km$^2$; the forest area decreased from 55.1% to 52.2% of the total basin with an annual deforestation rate of 0.2%. The fastest period of forest loss occurred during 2010–2020 with a decrease of 7988.5 km$^2$, followed by 1990–2000 (7391.3 km$^2$) and 2000–2010 (3802.4 km$^2$). At the sub-basin scale, the rate of deforestation in the DA is quite astonishing; the forest coverage rate decreased from 54.1% in 1990 to 46.7% in 2020, and more than 10,000 km$^2$ of forest were deforested during 1990–2000. In the UA, the area of forest also showed a continuing decline, but the rate of decline has been slowing down. The area of deforestation was only 295.0 km$^2$ during 2010–2020, which was 15.4% and 27.9% of that during 1990–2000 and 2000–2010, respectively. The forest area in the MA increased by 3454.4 km$^2$, compared to 1990. However, increases in the MA mainly occurred before 2000, after which the forest area slightly decreased.

### 3.2. Analysis of Dynamic Degree of LULCCs in the MRB

From 1990 to 2020, the comprehensive dynamic degree of LULCCs in the MRB was approximately 0.7%, and the most active period (1.4%) was during 1990–2000. From the perspective of a single dynamic degree of LULCCs, construction land, cropland, and forest were significantly different (Figure 2a). Among them, the single dynamic degree of construction land was 4.6%, indicating rapid expansion. In particular, the DA expansion trend was the most obvious, in which the single dynamic degree reached a high of 12.1%. The single dynamic degree of cropland was the largest (0.5%) in the DA, while it was −0.2% in the MA. In contrast, the forest single dynamic degree was −0.5% and 0.2% in the DA and MA, respectively. These values show that cropland expansion was often accompanied by forest loss, and cropland fallow was the main form of forest restoration in the MRB.

There are obvious differences in the single dynamic degrees of different types of LULCCs during different periods. From 1990 to 2000, the single dynamic degrees of construction land, cropland, and forest in the MRB are 3.7%, 0.2%, and −0.2%, respectively (Figure 2b). Among them, the expansion of construction land is the fastest in the DA, with a single dynamic degree of 8.8%, which is 5.1% and 6.1% higher than those of the UA and MA, respectively. Meanwhile, the single dynamic degree values of cropland were 0.4% and 0.9% in the UA and DA, respectively. The single dynamic degree of cropland in the MA was −0.5%. Correspondingly, the single dynamic degree of forest was less than 0 in the UA (−0.1%) and DA (−0.7%), while it was 0.7% in the MA.
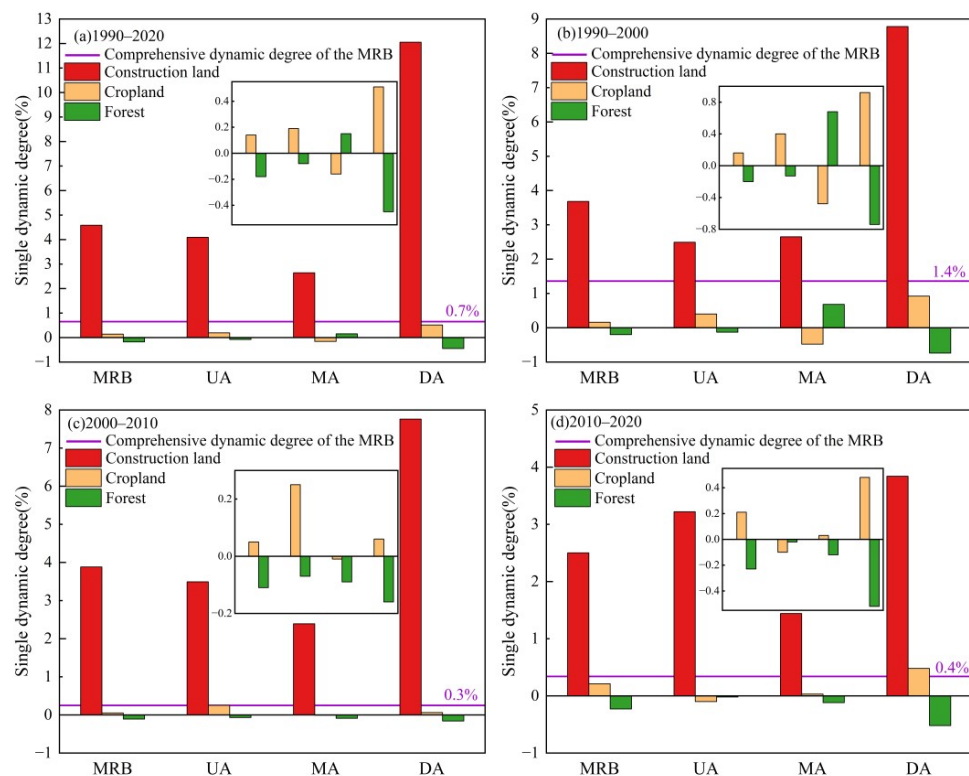
**Figure 2.** Dynamic degrees of land-use and land-cover changes in the Mekong River Basin (MRB) and its upstream area (UA), midstream area (MA), and downstream area (DA) during (**a**) 1990–2020, (**b**) 1990–2000, (**c**) 2000–2010, and (**d**) 2010–2020.

Compared with 1990–2000, the single dynamic degree of construction land was almost the same value (3.9%) during 2000–2010, still indicating rapid expansion (Figure 2c). In particular, the single dynamic degree of construction land in the DA was as high as 7.8%, much higher than that in the UA (3.5%) and MA (2.4%). However, the cropland expansion speed decreased, with a single dynamic degree of 0.1%, and the largest value was found in the UA (0.4%). The single dynamic degree of the forest was −0.1% and the rate of forest loss was also less pronounced than in the previous period, benefitting from the slower rate of cropland expansion. This is especially obvious in the DA, where the single dynamic degree changed from −0.7% in 1990–2000 to −0.2% in 2000–2010.

During 2010–2020, the single dynamic degree of construction land was 3.2% in the UA, while the cropland showed a decreasing trend for the first time, and the forest dynamic did not change much (Figure 2d). The single dynamic degree of construction land was the lowest (1.4%) in the MA, and the dynamic degrees of cropland and forest were not obvious in the MA. The single dynamic degree of construction land in the DA was 5.0% and 4.0% lower than those during 1990–2000 and 2000–2010, respectively. The single dynamic degree values of cropland and forest were 0.5% and −0.5% in the DA during the last period, respectively.

### 3.3. Analysis of Land-Use Transfer in the MRB

Based on geographic information system (GIS) overlay analysis, the land-use transfer processes during 1990–2020 (including the different stages) are shown in Figure 3. The key features of land-use transfer were the interconversions of forest and cropland, and cropland converted into construction land in the MRB. In addition, there was also a certain mutual transfer between cropland and water and wetland. Details of land-use transfer in the MRB from 1990 to 2020 can be found in Tables A2–A4.
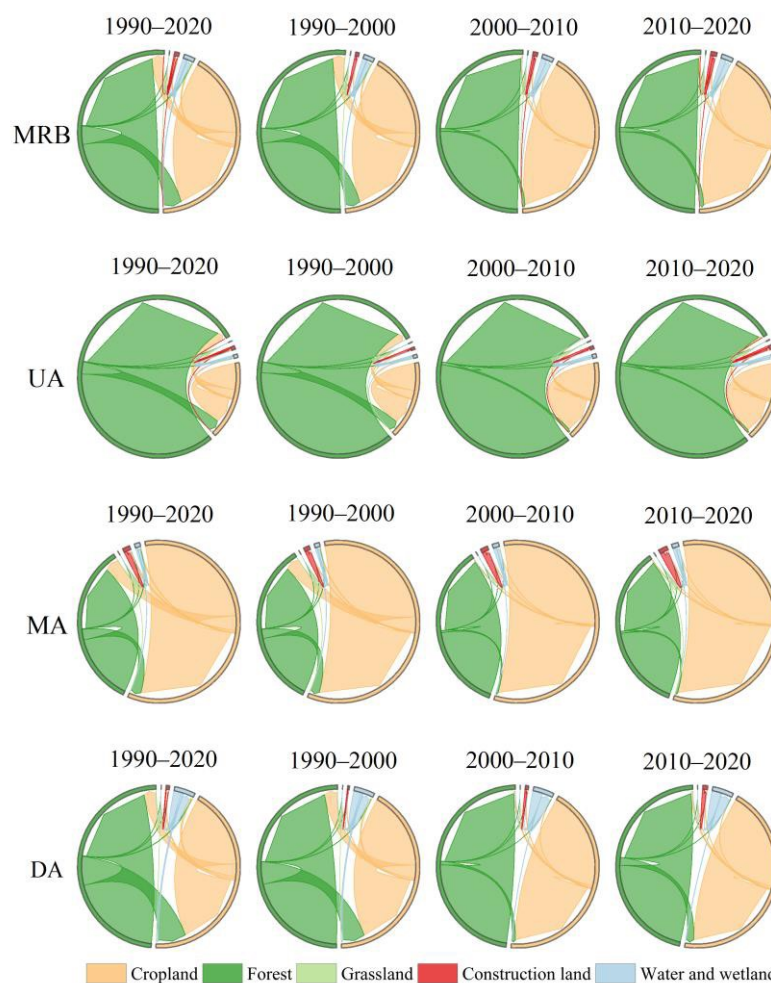
**Figure 3.** Land-use transfer in the Mekong River Basin (MRB) and its upstream area (UA), midstream area (MA), and downstream area (DA) during 1990–2020, 1990–2000, 2000–2010, and 2010–2020. Note that the arrows indicate the direction of transfer, and the width indicates the amount of transfer.

During 1990–2000, there were 88,888.3 km$^2$ of transferred land-use types in the MRB, accounting for 13.6% of the total land area. The area transferred from forest was 44,407.36 km$^2$, and 97.2% of that was transferred to cropland. Among them, about 88.0% of cropland (41,166.5 km$^2$) was converted into forest, followed by 8.7% of water and wetland and 3.3% of construction land. The area of water and wetland converted to other land-use types was 3217.5 km$^2$, of which 77.2% and 22.7% were converted into cropland and forest. A total of 73.8 km$^2$ of grassland was transferred out, of which 75.2% and 23.2% were transferred to forest and cropland. From 2000 to 2010, the area transferred from forest was 7964.9 km$^2$, of which 95.7% was transferred to cropland. The area transferred from cropland was 7174.9 km$^2$, of which 61.3%, 27.1%, and 11.6% were transferred to forest, construction land, and water and wetland, respectively. The water and wetland transferred out accounted for 555.1 km$^2$, of which 88.5% was converted to cropland. Of the grassland transferred out, 89.1% (70.1 km$^2$) was converted into forest. During 2010 to 2020, the area transferred from forest was 13,471.5 km$^2$, 95.7% of which was transferred to cropland. The area transferred from cropland was 7790.2 km$^2$, of which 68.6%, 21.1%, and 10.2% were converted into forest, construction land, and water and wetland, respectively. A total of 924.9 km$^2$ of water and wetland were transferred out, of which 86.0% was transferred to cropland. A total of 87.6% (63.2 km$^2$) of transferred-out grassland was converted into forest.

At the three sub-basins, although the major land-use transfer direction was similar, there were considerable differences in the quantities and characteristics. In the UA, the areas of land-use transfer were 15,725.1 km$^2$, 3859.6 km$^2$, and 4205.3 km$^2$, respectively, in the

past three periods. From 1990 to 2000, cropland was mainly transferred to forest, water and wetland, and construction land, with 6561.5 km$^2$, 355.9 km$^2$, and 179.1 km$^2$, respectively. The area transferred from forest was 8513.7 km$^2$, of which 96.1% was transferred to cropland. From 2000 to 2010, 1124.2 km$^2$ and 319.8 km$^2$ of cropland were converted into forest and construction land, and 2166.2 km$^2$ of forest was transferred to cropland. From 2010 to 2020, the transfer into construction land area was 448.5 km$^2$, of which 79.6% and 19.9% came from cropland and forest, respectively. The mutual conversion between cropland and forest was roughly the same, 1636.6 km$^2$ (i.e., from cropland to forest) and 1763.4 km$^2$ (i.e., from forest to cropland), respectively.

Next, the land-use transfer area in the MA was greater than in the UA in the past three periods. From 1990 to 2000, 14,321.6 km$^2$ and 612.0 km$^2$ of cropland were transferred to forest and construction land, respectively, and 8971.2 km$^2$ of forest were converted into cropland. From 2000 to 2010, 2169.9 km$^2$ of cropland was converted to other land-use types, and accounting for 56.5% of forest and 32.8% of construction land, respectively. The area transferred from forest was 1827.4 km$^2$, of which 92.6% was transferred to cropland. From 2010 to 2020, 1148.7 km$^2$ and 513.3 km$^2$ of cropland were transferred to forest and construction land, respectively, and 1982.7 km$^2$ of forest were converted into cropland.

The DA experienced the most dramatic land-use transfer, of which the area was more than the sum of the transfers in the UA and MA. From 1990 to 2000, 15,346.4 km$^2$ and 560.9 km$^2$ of cropland were transferred to forest and construction land, respectively. The trend of forest conversion to cropland was more obvious, with a total of 26,082.6 km$^2$ of forest converted to cropland. From 2010 to 2020, 3519.2 km$^2$ of cropland were converted to other land-use types, such as forest. Among them, about 58.1% and 26.0% were converted into forest and construction land, respectively. A total of 4135.0 km$^2$ of forest were converted to other types, of which 96.0% was converted into cropland. From 2010 to 2020, about 2558.0 km$^2$ and 733.0 km$^2$ of cropland were transferred to forest and construction land, respectively, and 9051.7 km$^2$ of forest were converted into cropland. Clearly, from forest to cropland is the most important land-use transfer in the DA.

### 3.4. Characteristics of Conflicts between Cropland and Forest

During 1990–2020, the conflicts between cropland and forest were the most obvious LULCCs, accounting for 86.4% of the total land-use transfer area in the MRB. Overall, cropland expansion and forest loss (CEFL) was more dominant in the DA (Figure 4a), while cropland fallow and forest restoration (CFFR) had an advantage in the MA. As shown in Figure 4b, the conflicts between cropland and forest were the most dramatic during 1990–2000. Before 2000, the ratios of CEFL in the UA, MA, and DA were 18.9%, 20.7%, and 60.6%, respectively. Meanwhile, the ratios of CFFR in the UA, MA, and DA were 18.1%, 39.5%, and 42.4%, respectively. The CEFL were 1615.9 km$^2$ and 10,736.2 km$^2$ more than the areas of CFFR in the UA and DA, respectively, whereas the areas of CFFR were 5404.4 km$^2$ more than those of CEFL in the MA. Compared with the period during 1990–2000, the conflicts between cropland and forest greatly decreased during 2000–2010 (Figure 4c). The ratios of CEFL in the UA, MA, and DA were 27.2%, 22.9%, and 49.9% in the first decade of the 21st century, respectively. Similarly, the ratios of CFFR in the UA, MA, and DA were 25.6%, 27.9%, and 46.5%, respectively. The areas of CEFL were 1042.0 km$^2$, 601.1 km$^2$, and 1927.1 km$^2$ more than those of CFFR in the UA, MA, and DA, respectively. During the latest period (2010–2020), the trend of CEFL was more prominent, especially in the DA, where 70.7% of the total changes in the MRB occurred (Figure 4d). The areas of CEFL were 6493.7 km$^2$ more than those of CFFR in the DA, but were only 126.8 km$^2$ and 834.1 km$^2$, respectively, in the UA and MA.
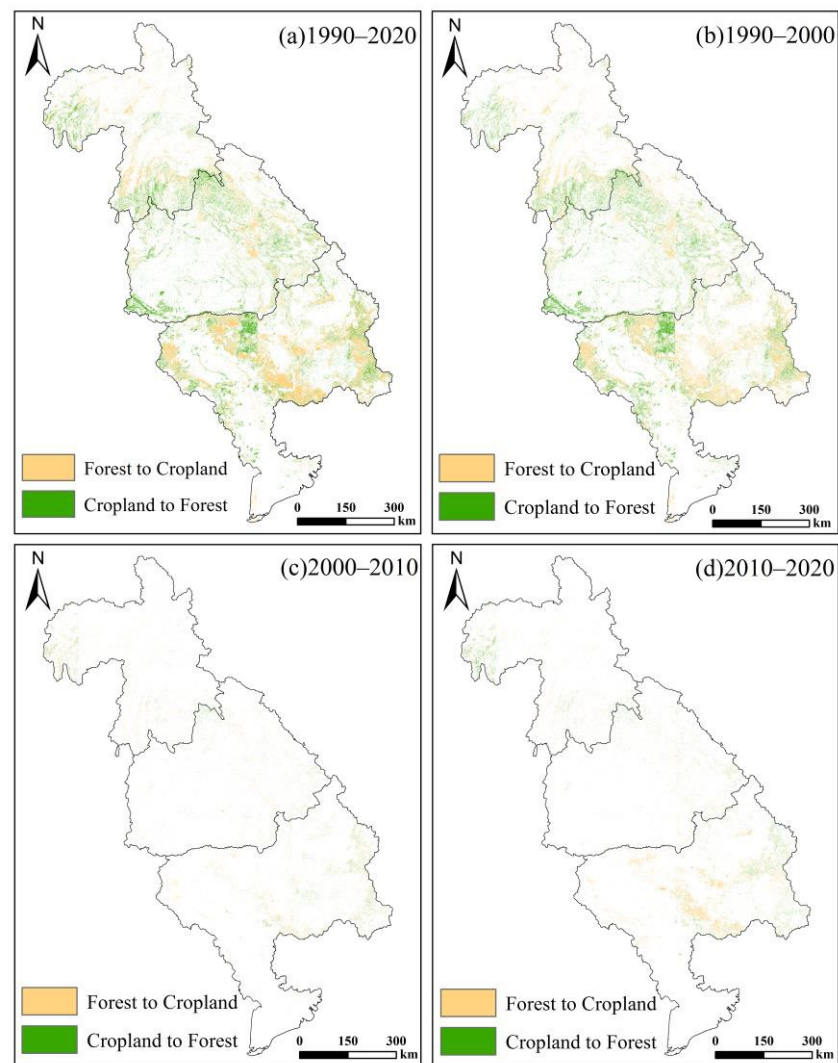
**Figure 4.** Spatial distributions of the conflicts between cropland and forest in the Mekong River Basin (MRB) during (**a**) 1990–2020, (**b**) 1990–2000, (**c**) 2000–2010, and (**d**) 2010–2020.

We also found that the conflicts between cropland and forest varied greatly among different elevations in the MRB in the last 31 years (Figure 5a). Specifically, about 60.0% and 23.1% of the CEFL occurred in the plains and hills, respectively. During 1990–2000, 61.4% of the CEFL was in the plains below 200 m. Then, although the scale of CEFL was decreasing during 2000–2010, the corresponding proportion of changes in the plains was still close to half (49.5%). Since 2010, about 68.8% of CEFL was located in the plains. This indicates that the forests in the plains were preferentially cut down and reclaimed as cropland. By contrast, CFFR obviously tend to be in areas with higher elevations that are unsuitable for cultivation. The proportion of CFFR in the plains decreased from 56.8% during 1990–2000 to 38.9% during 2010–2020, while the proportion increased from 11.4% to 30.2% in the low and middle mountains. It should be emphasized that the plains of the MRB account for the highest proportion of total land area, which is greater than the sum of the areas of other terrains. This further indicated that CFFR tends to occur in the highlands.
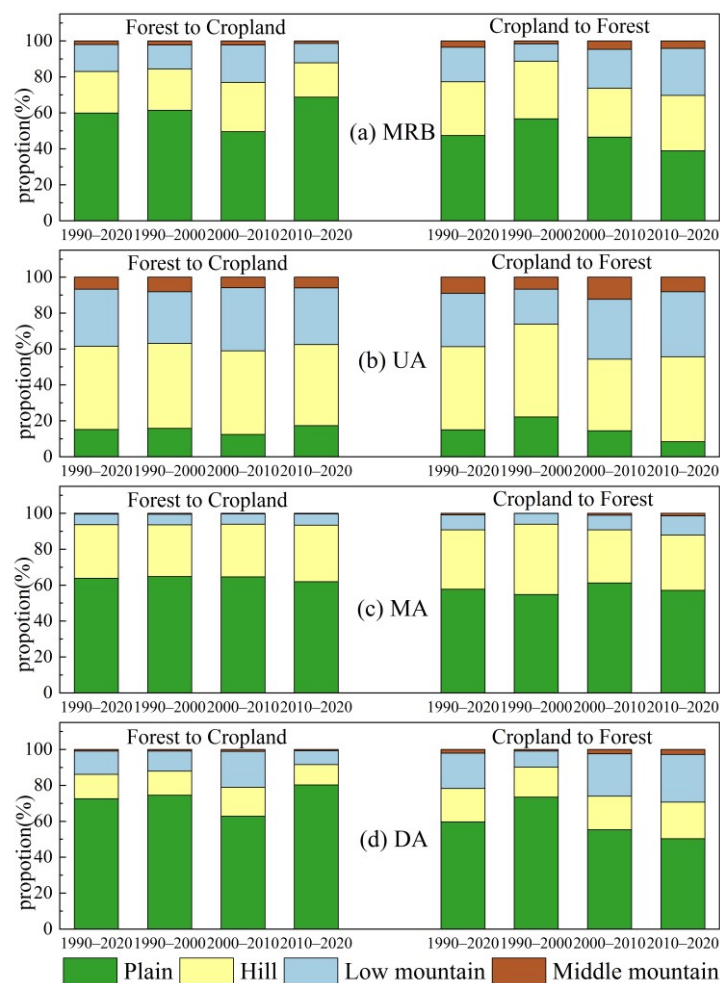
**Figure 5.** The proportion of conflicts between cropland and forest at different elevation gradients in the (**a**) Mekong River Basin (MRB) and its (**b**) upstream area (UA), (**c**) midstream area (MA), and (**d**) downstream area (DA) during 1990–2020, 1990–2000, 2000–2010, and 2010–2020.

Because the elevation differences of the three sub-basins are relatively significant, the elevation distributions of conflicts between cropland and forest also have distinct characteristics. The conflicts between cropland and forest in the UA mainly occurred in the hills and low mountains (Figure 5b), accounting for 76.0% during 1990–2000, 86.7% during 2000–2010, and 76.7% during 2010–2020, respectively. In particular, CFFR in the plains continued to decline, and tended to occur in higher elevation areas. In the MA, the conflicts between cropland and forest mainly occurred in the plains and hills (Figure 5c). The larger proportion of CFFR also tended to occur in the highlands; especially during the latest period (2010–2020), CFFR exceeded 10% in the low mountains for the first time. The conflicts between cropland and forest had the most obvious elevation change in the DA (Figure 5d). The CEFL was mainly occurred in the plains, resulting in 74.6%, 62.9%, and 80.3% of the changes during the three periods, respectively. Meanwhile, CFFR in the plains decreased from 73.5% during 1990–2000 to 50.3%, while the proportions increased from 9.9% to 29.3% in the low and middle mountains

## 4. Discussion

Tropical forests are a major source of new agricultural land [48]. Since the 1990s, rapid cropland expansion in MSEA is often associated with large-scale deforestation, including in the MRB [49]. The MRB has experienced rapid population growth over the past few decades [50], with the accompanying increased consumption of food, while the original cropland resources are limited. To balance the contradiction between the demand for food

and the supply of cropland, a large quantity of forest land has been cleared and reclaimed as cropland [51]. Comparatively speaking, cropland fallow and forest restoration (CFFR) receive less attention than cropland expansion and forest loss (CEFL), which account for a large proportion of LULCCs in the MRB and produce conflicts between cropland and forest. A series of policies to protect forests have been implemented in Thailand since 1989, such as the ban on logging of natural forests, because excessive deforestation led to severe flooding in 1988 [52]. Protected areas established and maintained by the Thai government cover approximately 19% of the country's land area in 2020 [53]. Our study shows that the trend of CEFL is the weakest and that of CFFR is the most obvious in the MA, which confirms that these measures are effective. Although a considerable amount of cropland has been restored to forests in the MRB, there is still a wide gap between forest restoration and forest loss. In general, when deforestation is greater than forest regeneration, forest patches become more isolated, which can affect regional biodiversity [54]. More importantly, tropical deforestation accounts for a large proportion of anthropogenic carbon emissions and has a profound impact on global climate change [55]. Therefore, controlling forest loss and accelerating forest regeneration should be given urgent attention under the umbrella of carbon peaking and carbon neutrality goals.

In the MRB, low-elevation areas are hot spots for LULCCs, especially those of CEFL, but these changes have gradually expanded to higher elevation areas [56]. Gradual highland CEFL in MSEA are also a cause for concern [57]. In addition, we found that the main area in which CFFR occurred was in the highlands in the MRB, which is similar to patterns in the rest of the world. For example, cropland returned to forest mainly occurred on sloping highlands in the Loess Plateau of China [58], Latin America, and the Caribbean [59]. In general, the advancement of agricultural technology has led to widespread deforestation in the lowlands, so highlands are the best places for forest restoration [60].

In fact, LULCCs are the result of a combination of factors, such as climate, topography, population, economy, policies, and institutions, which have been widely discussed in previous studies [61–65]. These factors are also the reasons for LULCCs in the MRB [66]. More importantly, geopolitical and economic relations are also the driving forces of LULCCs, but they are not well explained [67–69]. MRB countries have established more than 40 geopolitical and economic relationships with nonregional countries, which have profoundly affected the LULCCs in the region. The geopolinomical impact of LULCCs and the response of LULCCs to geopolinomical relationships have not been thoroughly studied. In the future, more attention should be paid to the role of geopolinomical relationships in LULCCs.

There were several limitations in this study. The division of our study area included multiple countries in the same sub-basin. However, the national differences were not well represented. In particular, national policy may play an important role in the LULCCs of MSEA's five countries, such as the afforestation (e.g., *acacia mangium*) movement in Vietnam [70] and the constriction of swidden agriculture in Laos [71]. Therefore, analyzing the differences in land-use policies across countries can help us to understand the reasons behind LULCCs in the MRB better. Additionally, more advanced models can be used for research in the future, which can not only better reveal past LULCCs, but can also predict future trends.

## 5. Conclusions

This study used 30 m land-use and ASTER GDEM V3 data and GIS methods via raster iterators and overlay analysis to examine the spatio-temporal characteristics of LULCCs and conflicts between cropland and forest in the MRB and its three sub-basins during 1990–2020, namely, the upstream area (UA), midstream area (MA), and downstream area (DA). Our basin-scale study can enrich the existing pan-regional results of LULCCs. The four main conclusions are as follows:

(1) From 1990 to 2020, the main LULCCs in the MRB were the continuous expansion of construction land and cropland, and the continuous loss of forest. Construction land and cropland increased by 5438.2 km$^2$ and 11,626.3 km$^2$, respectively, and forest de-

creased by 19,182.2 km$^2$. However, there are obvious differences in the performances in different periods and sub-basins.

(2) The LULCCs were the most active before 2000; the comprehensive dynamic degree of LULCCs was 1.4% in this period, and then it became relatively slight. The construction land expansion trend in the DA was the most obvious, and the single dynamic degree reached a high of 12.1%. The single dynamic degree of cropland was the largest (0.5%) in the DA, while it was −0.2% in the MA. In contrast, the single dynamic degrees of forest were −0.5% and 0.2% in the DA and MA, respectively.

(3) The key features of land-use transfer were the interconversion of forest and cropland, as well as cropland converted into construction land. More than 90% of the increased construction land was obtained from cropland, and a total of 17.7% of forest was reclaimed to cropland; meanwhile, 16.7% of cropland was returned to forest. Overall, the area of forest converted into cropland was greater than the area of cropland converted into forest.

(4) The conflict between croplands and forests is the most obvious LULCC, accounting for 86.4% of the MRB's totality. Cropland fallow and forest restoration (CFFR) was more obvious in the MA, and cropland expansion and forest loss (CEFL) had an advantage in the DA. Indeed, CEFL was mainly seen in the low-altitude plains below 200 m; it had the highest proportion during 2010–2020, reaching 68.8%. However, the proportion of CFFR in the plains decreased from 56.8% during 1990–2000 to 38.9% during 2010–2020, while the proportion increased from 11.4% to 30.2% in low- and middle-mountain areas above 500 m.

As noted, our study does not fully present a discussion of the drivers and mechanisms of LULCCs in the MRB. In the future, a long-time series of annual land-use practices will facilitate the understanding of the dynamics and related mechanisms of land-use changes. With the free access to satellite imagery, such as Landsat (including newly launched Landsat-9) and Sentinel, more efforts are needed to investigate the conflicts between croplands and forests, so as to investigate the reasons, mechanisms, and impacts an related to them.

**Author Contributions:** Conceptualization: C.X. and Y.L.; methodology: J.Z. and C.X.; software: J.Z.; validation: C.X. and Y.L.; resources: C.X.; writing—original draft preparation: J.Z.; writing—review and editing: C.X.; visualization: J.Z., Y.L., C.X. and Z.F.; supervision: Y.L. and C.X.; funding acquisition: C.X. and Z.F. All authors have read and agreed to the published version of the manuscript.

**Data Availability Statement:** Not applicable.

**Conflicts of Interest:** The authors declare no conflict of interest.

## Appendix A

**Table A1.** Area (km$^2$) of land use in the Mekong River Basin (MRB) from 1990 to 2020.

| Region | Land-Use and Land-Cover Types | 1990 | 2000 | 2010 | 2020 |
|---|---|---|---|---|---|
| MRB | Cropland | 275,541.0 | 280,024.0 | 281,312.7 | 287,167.3 |
| | Forest | 361,091.7 | 353,700.5 | 349,898.1 | 341,909.6 |
| | Grassland | 113.4 | 327.3 | 282.8 | 249.6 |
| | Construction land | 3957.4 | 5414.3 | 7516.1 | 9395.6 |
| | Water and wetland | 14,578.3 | 15,815.7 | 16,272.1 | 16,559.1 |

**Table A1.** *Cont.*

| Region | Land-Use and Land-Cover Types | 1990 | 2000 | 2010 | 2020 |
|--------|------------------------------|------|------|------|------|
| UA | Cropland | 27,789.3 | 28,910.5 | 29,633.2 | 29,350.6 |
| | Forest | 143,819.9 | 141,902.1 | 140,846.5 | 140,551.5 |
| | Grassland | 39.0 | 221.7 | 176.2 | 139.0 |
| | Construction land | 824.5 | 1029.4 | 1388.6 | 1836.2 |
| | Water and wetland | 1032.1 | 1441.1 | 1460.2 | 1626.9 |
| MA | Cropland | 139,015.4 | 132,367.3 | 132,170.4 | 132,533.6 |
| | Forest | 74,926.3 | 80,002.2 | 79,312.3 | 78,380.7 |
| | Grassland | 74.0 | 100.0 | 100.7 | 103.4 |
| | Construction land | 2444.5 | 3091.9 | 3830.5 | 4381.4 |
| | Water and wetland | 2054.2 | 2952.9 | 3100.4 | 3115.2 |
| DA | Cropland | 108,736.3 | 118,746.1 | 119,509.2 | 125,283.2 |
| | Forest | 142,345.6 | 131,796.2 | 129,739.2 | 122,977.3 |
| | Grassland | 0.4 | 5.6 | 5.9 | 7.2 |
| | Construction land | 688.5 | 1293.1 | 2297.0 | 3178.0 |
| | Water and wetland | 11,492.1 | 11,421.7 | 11,711.5 | 11,817.1 |

**Table A2.** The transfer matrix of land-use changes in the Mekong River Basin from 1990 to 2000 (km$^2$).

| 1990 | 2000 | | | | |
|------|----------|--------|-----------|-------------------|------------------|
| | Cropland | Forest | Grassland | Construction Land | Water and Wetland |
| Cropland | 234,351.4 | 36,229.5 | 23.0 | 1352.0 | 3585.0 |
| Forest | 43,177.2 | 316,684.4 | 262.2 | 103.5 | 864.4 |
| Grassland | 12.8 | 55.4 | 39.6 | 0.1 | 5.5 |
| Construction land | 0.0 | 0.0 | 0.0 | 3957.4 | 0.0 |
| Water and wetland | 2482.5 | 731.3 | 2.5 | 1.3 | 11,360.8 |

**Table A3.** The transfer matrix of land-use changes in the Mekong River Basin from 2000 to 2010 (km$^2$).

| 2000 | 2010 | | | | |
|------|----------|--------|-----------|-------------------|------------------|
| | Cropland | Forest | Grassland | Construction Land | Water and Wetland |
| Cropland | 272,849.0 | 4394.7 | 2.5 | 1946.0 | 831.7 |
| Forest | 7964.9 | 345,373.5 | 31.4 | 150.9 | 179.8 |
| Grassland | 7.9 | 70.1 | 248.6 | 0.7 | 0.0 |
| Construction land | 0.0 | 0.0 | 0.0 | 5414.3 | 0.0 |
| Water and wetland | 490.9 | 59.8 | 0.2 | 4.1 | 15,260.7 |

**Table A4.** The transfer matrix of land-use changes in the Mekong River Basin from 2010 to 2020 (km$^2$).

| 2010 | 2020 | | | | |
|------|----------|--------|-----------|-------------------|------------------|
| | Cropland | Forest | Grassland | Construction Land | Water and Wetland |
| Cropland | 273,522.5 | 5343.2 | 7.6 | 1643.4 | 795.5 |
| Forest | 12,797.8 | 336,426.6 | 29.8 | 227.8 | 416.1 |
| Grassland | 7.5 | 63.2 | 210.6 | 1.2 | 0.2 |
| Construction land | 0.8 | 0.1 | 0.0 | 7515.1 | 0.0 |
| Water and wetland | 838.8 | 76.4 | 1.7 | 8.0 | 15,347.3 |

## References

1. Salazar, A.; Baldi, G.; Hirota, M.; Syktus, J.; McAlpine, C. Land use and land cover change impacts on the regional climate of non-Amazonian South America: A review. *Glob. Planet. Change* **2015**, *128*, 103–119. [CrossRef]
2. Nie, W.; Yuan, Y.; Kepner, W.; Nash, M.S.; Jackson, M.; Erickson, C. Assessing impacts of Landuse and Landcover changes on hydrology for the upper San Pedro watershed. *J. Hydrol.* **2011**, *407*, 105–114. [CrossRef]
3. Pal, S.; Ziaul, S. Detection of land use and land cover change and land surface temperature in English Bazar urban centre. *Egypt. J. Remote Sens. Space Sci.* **2017**, *20*, 125–145. [CrossRef]
4. Tran, D.X.; Pla, F.; Latorre-Carmona, P.; Myint, S.W.; Gaetano, M.; Kieu, H.V. Characterizing the relationship between land use land cover change and land surface temperature. *ISPRS J. Photogramm. Remote Sens.* **2017**, *124*, 119–132. [CrossRef]
5. Li, Z.T.; Li, M.; Xia, B.C. Spatio-temporal dynamics of ecological security pattern of the Pearl River Delta urban agglomeration based on LUCC simulation. *Ecol. Indic.* **2020**, *114*, 106319. [CrossRef]
6. Chuai, X.; Huang, X.; Wang, W.; Zhao, R.; Zhang, M.; Wu, C. Land use, total carbon emission's change and low carbon land management in Coastal Jiangsu, China. *J. Cleaner Prod.* **2015**, *103*, 77–86. [CrossRef]
7. Fu, B.; Wu, M.; Che, Y.; Yang, K. Effects of land use changes on city-level net carbon emissions based on a coupled model. *Carbon Manag.* **2017**, *8*, 245–262. [CrossRef]
8. Ding, Y.; Feng, H.; Zou, B.; Ye, S. Contribution Isolation of LUCC Impact on Regional PM2.5 Air Pollution: Implications for Sustainable Land and Environment Management. *Front. Environ. Sci.* **2022**, *10*, 825732. [CrossRef]
9. Zhang, F.; Yushanjiang, A.; Wang, D. Ecological risk assessment due to land use/cover changes (LUCC) in Jinghe County, Xinjiang, China from 1990 to 2014 based on landscape patterns and spatial statistics. *Environ. Earth Sci.* **2018**, *77*, 491. [CrossRef]
10. Wu, K.; Ye, X.; Qi, Z.; Zhang, H. Impacts of land use/land cover change and socioeconomic development on regional ecosystem services: The case of fast-growing Hangzhou metropolitan area, China. *Cities* **2013**, *31*, 276–284. [CrossRef]
11. Hak, T.; Janouskova, S.; Moldan, B. Sustainable Development Goals: A need for relevant indicators. *Ecol. Indic.* **2016**, *60*, 565–573. [CrossRef]
12. Hosonuma, N.; Herold, M.; De Sy, V.; De Fries, R.S.; Brockhaus, M.; Verchot, L.; Angelsen, A.; Romijn, E. An assessment of deforestation and forest degradation drivers in developing countries. *Environ. Res. Lett.* **2012**, *7*, 044009. [CrossRef]
13. Cao, Q.; Yu, D.; Georgescu, M.; Han, Z.; Wu, J. Impacts of land use and land cover change on regional climate: A case study in the agro-pastoral transitional zone of China. *Environ. Res. Lett.* **2015**, *10*, 124025. [CrossRef]
14. Pelorosso, R.; Leone, A.; Boccia, L. Land cover and land use change in the Italian central Apennines: A comparison of assessment methods. *Appl. Geogr.* **2009**, *29*, 35–48. [CrossRef]
15. Song, W.; Deng, X. land use/land cover change and ecosystem service provision in China. *Sci. Total Environ.* **2017**, *576*, 705–719. [CrossRef]
16. Xiao, D.; Niu, H.; Guo, J.; Zhao, S.; Fan, L. Carbon Storage Change Analysis and Emission Reduction Suggestions under Land Use Transition: A Case Study of Henan Province, China. *Int. J. Environ. Res. Public Health* **2021**, *18*, 1844. [CrossRef]
17. He, C.; Zhang, J.; Liu, Z.; Huang, Q. Characteristics and progress of land use/cover change research during 1990–2018. *J. Geogr. Sci.* **2022**, *32*, 537–559. [CrossRef]
18. Velazquez, A.; Duran, E.; Ramirez, I.; Mas, J.F.; Bocco, G.; Ramirez, G.; Palacio, J.L. Land use-cover change processes in highly biodiverse areas: The case of Oaxaca, Mexico. *Glob. Environ. Chang.* **2003**, *13*, 175–184. [CrossRef]
19. Ning, J.; Liu, J.; Kuang, W.; Xu, X.; Zhang, S.; Yan, C.; Li, R.; Wu, S.; Hu, Y.; Du, G.; et al. Spatiotemporal patterns and characteristics of land use change in China during 2010–2015. *J. Geogr. Sci.* **2018**, *28*, 547–562. [CrossRef]
20. Tong, S.; Bao, G.; Rong, A.; Huang, X.; Bao, Y.; Bao, Y. Comparison of the Spatiotemporal Dynamics of Land Use Changes in Four Municipalities of China Based on Intensity Analysis. *Sustainability* **2020**, *12*, 3687. [CrossRef]
21. Li, X.Y.; Ma, Y.J.; Xu, H.Y.; Wang, J.H.; Zhang, D.S. Impact of land use and land cover change on environmental degradation in lake Qinghai watershed, northeast Qinghai-Tibet Plateau. *Land Degrad. Dev.* **2009**, *20*, 69–83. [CrossRef]
22. Wasige, J.E.; Groen, T.A.; Smaling, E.; Jetten, V. Monitoring basin-scale land cover changes in Kagera Basin of Lake Victoria using ancillary data and remote sensing. *Int. J. Appl. Earth Obs. Geoinf.* **2013**, *21*, 32–42. [CrossRef]
23. Wang, F.; Ge, Q.S.; Yu, Q.B.; Wang, H.X.; Xu, X.L. Impacts of land use and land cover changes on river runoff in Yellow River basin for period of 1956–2012. *Chin. Geogr. Sci.* **2017**, *27*, 13–24. [CrossRef]
24. Yang, H.F.; Zhong, X.N.; Deng, S.Q.; Xu, H. Assessment of the impact of LUCC on NPP and its influencing factors in the Yangtze River basin, China. *Catena* **2021**, *206*, 105542. [CrossRef]
25. Liu, B.; Pan, L.; Qi, Y.; Guan, X.; Li, J. Land Use and Land Cover Change in the Yellow River Basin from 1980 to 2015 and Its Impact on the Ecosystem Services. *Land* **2021**, *10*, 1080. [CrossRef]
26. Liu, J.; Zhang, Z.; Xu, X.; Kuang, W.; Zhou, W.; Zhang, S.; Li, R.; Yan, C.; Yu, D.; Wu, S.; et al. Spatial patterns and driving forces of land use change in China during the early 21st century. *J. Geogr. Sci.* **2010**, *20*, 483–494. [CrossRef]
27. Liu, J.Y.; Zhan, J.Y.; Deng, X.Z. Spatio-temporal patterns and driving forces of urban land expansion in china during the economic reform era. *Ambio* **2005**, *34*, 450–455. [CrossRef]
28. Sims, K. The Asian Development Bank and the production of poverty: Neoliberalism, technocratic modernization and land dispossession in the Greater Mekong Subregion. *Singap. J. Trop. Geogr.* **2015**, *36*, 112–126. [CrossRef]
29. Pech, S.; Sunada, K. Population growth and natural-resources pressures in the Mekong River Basin. *Ambio A J. Hum. Environ.* **2008**, *37*, 219–224. [CrossRef]

30. Cao, H.; Liu, J.; Chen, J.; Gao, J.; Wang, G.; Zhang, W. Spatiotemporal Patterns of Urban Land Use Change in Typical Cities in the Greater Mekong Subregion (GMS). *Remote Sens.* **2019**, *11*, 801. [CrossRef]

31. Li, P.; Feng, Z.; Xiao, C.; Khampheng, B.; Liu, Y. Detecting and mapping annual newly-burned plots (NBP) of swiddening using historical Landsat data in Montane Mainland Southeast Asia (MMSEA) during 1988–2016. *J. Geogr. Sci.* **2018**, *28*, 1307–1328. [CrossRef]

32. Li, P.; Xiao, C.; Feng, Z. Swidden agriculture in transition and its roles in tropical forest loss and industrial plantation expansion. *Land Degrad. Deve.* **2022**, *33*, 388–392. [CrossRef]

33. Stibig, H.J.; Achard, F.; Carboni, S.; Rasi, R.; Miettinen, J. Change in tropical forest cover of Southeast Asia from 1990 to 2010. *Biogeosciences* **2014**, *11*, 247–258. [CrossRef]

34. Zheng, F.; Huang, J.; Feng, Z.; Xiao, C. Impact of the Kunming-Bangkok Highway on Land Use Changes along the Route between Laos and Thailand. *Land* **2021**, *10*, 991. [CrossRef]

35. Costa-Cabral, M.C.; Richey, J.E.; Goteti, G.; Lettenmaier, D.P.; Feldkotter, C.; Snidvongs, A. Landscape structure and use, climate, and water movement in the Mekong River basin. *Hydrol. Processes* **2008**, *22*, 1731–1746. [CrossRef]

36. Pan, M.; Yang, K. Analysis of Variation Characteristics and Driving Factors of Tonle Sap Lake's Surface Water Temperature from 2001 to 2018. *Pol. J. Environ. Stud.* **2021**, *30*, 2709–2722. [CrossRef]

37. Tromboni, F.; Dilts, T.E.; Null, S.E.; Lohani, S.; Ngor, P.B.; Soum, S.; Hogan, Z.; Chandra, S. Changing Land Use and Population Density Are Degrading Water Quality in the Lower Mekong Basin. *Water* **2021**, *13*, 1948. [CrossRef]

38. Jiang, P.H.; Cheng, L.; Li, M.C.; Zhao, R.F.; Duan, Y.W. Impacts of LUCC on soil properties in the riparian zones of desert oasis with remote sensing data: A case study of the middle Heihe River basin, China. *Sci. Total Environ.* **2015**, *506*, 259–271. [CrossRef]

39. Wang, H.; Sun, F.; Xia, J.; Liu, W. Impact of LUCC on streamflow based on the SWAT model over the Wei River basin on the Loess Plateau in China. *Hydrol. Earth Syst. Sci.* **2017**, *21*, 1929–1945. [CrossRef]

40. Zhan, C.S.; Xu, Z.X.; Ye, A.Z.; Su, H.B. LUCC and its impact on run-off yield in the Bai River catchment-upstream of the Miyun Reservoir basin. *J. Plant. Ecol.* **2011**, *4*, 61–66. [CrossRef]

41. Thilakarathne, M.; Sridhar, V. Characterization of future drought conditions in the Lower Mekong River Basin. *Weather. Clim. Extremes* **2017**, *17*, 47–58. [CrossRef]

42. Ziv, G.; Baran, E.; Nam, S.; Rodriguez-Iturbe, I.; Levin, S.A. Trading-off fish biodiversity, food security, and hydropower in the Mekong River Basin. *Proc. Natl. Acad. Sci. USA* **2012**, *109*, 5609–5614. [CrossRef] [PubMed]

43. Zhang, X.; Liu, L.; Chen, X.; Gao, Y.; Xie, S.; Mi, J. GLC_FCS30: Global land cover product with fine classification system at 30m using time-series Landsat imagery. *Earth Syst. Sci. Data* **2021**, *13*, 2753–2776. [CrossRef]

44. Wu, L.; Xie, B.; Xiao, X.; Xue, B.; Li, J. Classification Method and Determination of Mountainous Area Types at Township Scales: A Case Study of Yuxi City, Yunnan Province. *Complexity* **2020**, *2020*, 3484568. [CrossRef]

45. Zhang, B.; Fan, Z.; Du, Z.; Zheng, J.; Luo, J.; Wang, N.; Wang, Q. A Geomorphological Regionalization using the Upscaled DEM: The Beijing-Tianjin-Hebei Area, China Case Study. *Sci. Rep.* **2020**, *10*, 10532. [CrossRef]

46. Li, G.; Wang, J.; Wang, Y.; Wei, H.; Ochir, A.; Davaasuren, D.; Chonokhuu, S.; Nasanbat, E. Spatial and Temporal Variations in Grassland Production from 2006 to 2015 in Mongolia Along the China-Mongolia Railway. *Sustainability* **2019**, *11*, 2177. [CrossRef]

47. Zhang, F.; Kung, H.-t.; Johnson, V.C. Assessment of Land cover/Land-Use Change and Landscape Patterns in the Two National Nature Reserves of Ebinur Lake Watershed, Xinjiang, China. *Sustainability* **2017**, *9*, 724. [CrossRef]

48. Gibbs, H.K.; Ruesch, A.S.; Achard, F.; Clayton, M.K.; Holmgren, P.; Ramankutty, N.; Foley, J.A. Tropical forests were the primary sources of new agricultural land in the 1980s and 1990s. *Proc. Natl. Acad. Sci. USA* **2010**, *107*, 16732–16737. [CrossRef]

49. Lepers, E.; Lambin, E.F.; Janetos, A.C.; DeFries, R.; Achard, F.; Ramankutty, N.; Scholes, R.J. A synthesis of information on rapid land cover change for the period 1981–2000. *Bioscience* **2005**, *55*, 115–124. [CrossRef]

50. Yin, X.; Li, P.; Feng, Z.M.; Yang, Y.Z.; You, Z.; Xiao, C.W. Which Gridded Population Data Product Is Better? Evidences from Mainland Southeast Asia (MSEA). *ISPRS Int. J. Geoinf.* **2021**, *10*, 681. [CrossRef]

51. Xu, X.; Jain, A.K.; Calvin, K.V. Quantifying the biophysical and socioeconomic drivers of changes in forest and agricultural land in South and Southeast Asia. *Glob. Chang. Biol.* **2019**, *25*, 2137–2151. [CrossRef] [PubMed]

52. Buddharat, C.; Kaewkamjan, K.; Promchitta, V.; Phanon, W.; Sirirat, K.; Boonsuk, Y.; Sipaoraya, M. Tourism in phipun distract: From dark to dawn. *Int. J. Bus. Soc.* **2020**, *21*, 454–472. [CrossRef]

53. Singh, M.; Griaud, C.; Collins, C.M. An evaluation of the effectiveness of protected areas in Thailand. *Ecol. Indic.* **2021**, *125*, 107536. [CrossRef]

54. Lira, P.K.; Tambosi, L.R.; Ewers, R.M.; Metzger, J.P. land use and land cover change in Atlantic Forest landscapes. *For. Ecol. Manag.* **2012**, *278*, 80–89. [CrossRef]

55. Gibbs, H.K.; Herold, M. Tropical deforestation and greenhouse gas emissions. *Environ. Res. Lett.* **2007**, *2*, 045021. [CrossRef]

56. Wang, J.; Sui, L.C.; Yang, X.M.; Wang, Z.H.; Ge, D.Z.; Kang, J.M.; Yang, F.S.; Liu, Y.M.; Liu, B. Economic Globalization Impacts on the Ecological Environment of Inland Developing Countries: A Case Study of Laos from the Perspective of the Land Use/Cover Change. *Sustainability* **2019**, *11*, 3940. [CrossRef]

57. Zeng, Z.; Estes, L.; Ziegler, A.D.; Chen, A.; Searchinger, T.; Hua, F.; Guan, K.; Jintrawet, A.; Wood, E.F. Highland cropland expansion and forest loss in Southeast Asia in the twenty-first century. *Nat. Geosci.* **2018**, *11*, 556–562. [CrossRef]

58. Xu, X.; Ju, T.; Zheng, S. Sediment sources of Yan'gou watershed in the Loess Hilly region China under a certain rainstorm event. *Springerplus* **2013**, *2*, S2. [CrossRef]

59. Aide, T.M.; Clark, M.L.; Ricardo Grau, H.; Lopez-Carr, D.; Levy, M.A.; Redo, D.; Bonilla-Moheno, M.; Riner, G.; Andrade-Nunez, M.J.; Muniz, M. Deforestation and Reforestation of Latin America and the Caribbean (2001–2010). *Biotropica* **2013**, *45*, 262–271. [CrossRef]

60. Mueller, R.; Mueller, D.; Schierhorn, F.; Gerold, G.; Pacheco, P. Proximate causes of deforestation in the Bolivian lowlands: An analysis of spatial dynamics. *Reg. Environ. Chang.* **2012**, *12*, 445–459. [CrossRef]

61. Dong, S.; Li, Y.; Li, Y.; Li, S. Spatiotemporal Patterns and Drivers of Land Use and Land Cover Change in the China-Mongolia-Russia Economic Corridor. *Pol. J. Environ. Stud.* **2021**, *30*, 2527–2541. [CrossRef]

62. Gao, C.; Zhou, P.; Jia, P.; Liu, Z.; Wei, L.; Tian, H. Spatial driving forces of dominant land use/land cover transformations in the Dongjiang River watershed, Southern China. *Environ. Monit. Assess.* **2016**, *188*, 84. [CrossRef] [PubMed]

63. Hanh, T.; Quoc, N.; Kervyn, M. Factors influencing people's knowledge, attitude, and practice in land use dynamics: A case study in Ca Mau province in the Mekong delta, Vietnam. *Land Use Policy* **2018**, *72*, 227–238.

64. Li, K.; Feng, M.; Biswas, A.; Su, H.; Niu, Y.; Cao, J. Driving Factors and Future Prediction of Land Use and Cover Change Based on Satellite Remote Sensing Data by the LCM Model: A Case Study from Gansu Province, China. *Sensors* **2020**, *20*, 2757. [CrossRef] [PubMed]

65. Zhai, R.; Zhang, C.; Li, W.; Zhang, X.; Li, X. Evaluation of Driving Forces of Land Use and Land Cover Change in New England Area by a Mixed Method. *ISPRS Int. J. Geoinf.* **2020**, *9*, 350. [CrossRef]

66. Rowcroft, P. Frontiers of change: The reasons behind land use change in the Mekong Basin. *Ambio A J. Hum. Environ.* **2008**, *37*, 213–218. [CrossRef]

67. Cotula, L. The international political economy of the global land rush: A critical appraisal of trends, scale, geography and drivers. *J. Peasant Stud.* **2012**, *39*, 649–680. [CrossRef]

68. Woods, K.M.; Wang, P.; Sexton, J.O.; Leimgruber, P.; Wong, J.; Huang, Q. Integrating Pixels, People, and Political Economy to Understand the Role of Armed Conflict and Geopolitics in Driving Deforestation: The Case of Myanmar. *Remote Sens.* **2021**, *13*, 4589. [CrossRef]

69. Wu, S.S.; Chong, A. Developmental Railpolitics: The Political Economy of China's High-Speed Rail Projects in Thailand and Indonesia. *Contemp. Southeast. Asia* **2018**, *40*, 503–526.

70. Meyfroidt, P.; Lambin, E.F. Forest transition in Vietnam and displacement of deforestation abroad. *Proc. Natl. Acad. Sci. USA* **2009**, *106*, 16139–16144. [CrossRef]

71. Sovu; Tigabu, M.; Savadogo, P.; Ode'n, P.C.; Xayvongs, L. Recovery of secondary forests on swidden cultivation fallows in Laos. *For. Ecol. Manag.* **2009**, *258*, 2666–2675.